Inorganic Chemistry

Article

pubs.acs.org/IC

High-Pressure Synthesis and Superconductivity of the Laves Phase Compound $Ca(Al,Si)_2$ Composed of Truncated Tetrahedral Cages $Ca@(Al,Si)_{12}$

Masashi Tanaka, Shuai Zhang, Kei Inumaru, and Shoji Yamanaka*

Department of Applied Chemistry, Graduate School of Engineering, Hiroshima University, Higashi-Hiroshima 739-8527, Japan

Supporting Information

ABSTRACT: The Zintl compound $CaAl_2Si_2$ peritectically decomposes to a new ternary cubic Laves phase $Ca(Al,Si)_2$ and an Al−Si eutectic at temperatures above 750 °C under a pressure of 13 GPa. The ternary Laves phase compound can also be prepared as solid solutions $Ca(Al_{1-x}Si_x)_2$ ($0.35 \leq x \leq 0.75$) directly from the ternary mixtures under high-pressure and high-temperature conditions. The cubic Laves phase structure can be regarded as a type of clathrate compound composed of face-sharing truncated tetrahedral cages with Ca atoms at the center, $Ca@(Al,Si)_{12}$. The compound with a stoichiometric composition CaAlSi exhibits superconductivity with a transition temperature of 2.6 K. This is the first superconducting Laves phase compound composed solely of commonly found elements.

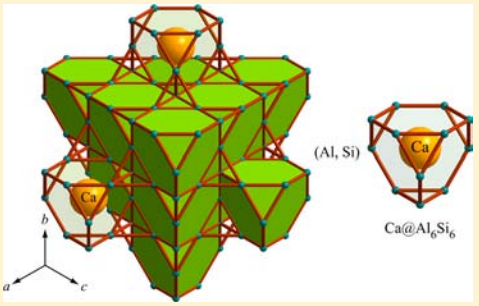

INTRODUCTION

Much attention has been paid to the synthesis of intermetallic compounds under high-pressure and high-temperature (HPHT) conditions, in particular, in binary and ternary systems containing strongly electropositive elements (A) such as alkali, alkaline-earth, and rare-earth metals, and covalent bond network formers (E) such as Si and Ge. Various types of new covalent subnetworks have been developed with unusual E/A atomic ratios, which violate the electron counting rule, according to the conventional Zintl concept. The compounds have unusual coordination environments and/or excess electrons in the networks. Note that most of them exhibit superconductivity. We have shown that the barium-containing type I silicon clathrate compound Ba_8Si_{46} can be obtained only under HPHT conditions,[1] which has been found to become a superconductor with a superconducting transition temperature of T_c = 8.0 K; this is the first superconductor that has a silicon clathrate network. In binary silicides under HPHT conditions, silicon-rich compounds are generated, such as $LaSi_5$ (T_c = 11.5 K), $LaSi_{10}$ (T_c = 6.7 K), $Ba_{24}Si_{100}$ (T_c = 1.4 K), $BaSi_6$, $SrSi_6$, and MSi_3 (M = Ca, Y, Lu; T_c = 4−7 K).[2−6] $LaSi_5$ contains one-dimensional sila-polyacene ribbons, i.e., Si ladder polymer.[2] For rare-earth germanides, $LnGe_5$ (Ln = La (T_c = 7.0 K), Ce, Pr, Nd, Sm, Gd, Tb) with a coordination number of CN = 8; more recently, $BaGe_3$ and $CaGe_3$ (T_c = 6.8 K) with CN = 6 have been reported.[7−10] These HPHT syntheses obey Le Chatelier's principle; the molar volume of the reactant of the system decreases in the product by forming developed covalent networks and high-coordination environments. Phase transitions under HPHT conditions also obey the same rule. For example, $SrSi_2$ is transformed to the layered $CaSi_2$ and the α-$ThSi_2$-type structure with reduced molecular volumes.[11] Mg_2Si with the antifluorite structure (CN = 8) is transformed to the anticotunnite structure (the $PbCl_2$-type, CN = 9), and then to the $InNi_2$-type structure (CN = 11) under a much higher pressure using a diamond anvil cell (DAC) at room temperature.[12,13] A solid solution $Mg_{2-x}Al_xSi$ ($0.3 < x < 0.8$) with the anticotunnite structure has been prepared under HPHT conditions, which has also been found to become a superconductor at T_c = 6.2 K when $x > 0.5$.[14]

In ternary compounds, the HPHT effect is more complicated. Ionic Zintl compounds melting congruently under ambient pressure decompose peritectically under high pressure. Recently, we have shown that a typical Zintl compound $CaAl_2Si_2$, which melts at 938 °C under ambient pressure, decomposes to a new ternary phase $Ca_2Al_3Si_4$ (superconductor with T_c = 6.2 K) at 5 GPa and ∼600 °C.[15] The new ternary compound consists of two types of interpenetrating subnetworks: the cagelike $[Al_3Si_4]$ and the layer structured $[Ca_2]$, which is isomorphous with black phosphorus. In this study, a much higher pressure is applied to $CaAl_2Si_2$. The compound undergoes a different type of decomposition, and a new ternary compound $Ca(Al,Si)_2$ with the cubic Laves phase structure has been obtained. The superconductivity of the ternary Laves phase compound is examined. This is a part of the studies to develop new superconductors composed of commonly found elements.

EXPERIMENTAL SECTION

High-Pressure and High-Temperature (HPHT) Synthesis. Calcium metal was purified prior to use by sublimation at 800 °C and deposition onto a water-cooled molybdenum plate under vacuum.[16] Calcium metal is very reactive and difficult to handle.

Received: February 15, 2013
Published: May 8, 2013

dx.doi.org/10.1021/ic400395n | Inorg. Chem. 2013, 52, 6039−6045

$CaSi_2$ was first prepared from a stoichiometric mixture of calcium metal and silicon (99.999%) by arc melting under an argon atmosphere. $CaSi_2$ was used as a source of calcium as well as silicon. $CaAl_2Si_2$ was prepared from a stoichiometric mixture of $CaSi_2$ and aluminum, using arc melting. The ternary mixtures with nominal compositions of $Ca(Al_{1-x}Si_x)_2$ ($0.15 \le x \le 0.75$) were premelted using an arc furnace, followed by remelting for 3 h at 1000−1200 °C using radio frequency (RF) induction heating under an argon atomosphere in an *h*-BN crucible with a cover. The ternary mixture with $x = 0.5$, was identified to be the layered compound CaAlSi isomorphous with AlB_2.[17] The cooled ternary mixtures were supplied for the HPHT treatment, which was carried out using a Kawai-type multianvil press.[18] The ground powders of $CaSi_2$, $CaAl_2Si_2$, and the ternary mixtures were separately loaded into a cylindrical *h*-BN cell (with an inner diameter of 1.5−3.0 mm and a depth of 3.5−4.6 mm). The *h*-BN cell was surrounded by a carbon tube heater and placed in a calcined pyrophllite tube for thermal insulation. The cell, in turn, was housed in a pierced Co-doped MgO octahedron. The assemblage was compressed in the multianvil apparatus with a truncation edge length of 4−6 mm up to 13−15 GPa and heated at 750−1000 °C for 1 h, followed by a rapid quenching to room temperature. The sample temperature was monitored and controlled using a chromel−alumel thermocouple.

Characterization. Single-crystal X-ray structural analysis was performed on a Rigaku Model AFC7R Mercury CCD diffractometer with Mo Kα radiation (λ = 0.71073 Å) coupled with CrystalClear interface (Rigaku) for data collection. The single-crystal structure was refined with the program SHELX97 and the WinGX software package.[19,20] Powder X-ray diffraction (XRD) patterns were measured by an imaging plate (IP) Guinier diffractometer (Huber, Model 670G) using Cu Kα_1 (λ = 1.540596 Å) radiation and a glass capillary goniometer. TOPAS-Academic software package was used for the Rietveld analysis.[21] The sample composition was determined by electron probe microanalysis (EPMA) (JEOL, Model JCMA-733II), using standards of $CaSiO_3$, Al_2O_3, and silicon for Ca, Al, and Si, respectively. Backscattered electron (BSE) images were observed by scanning electron microscopy (SEM) for microstructural analysis. Magnetic susceptibility was measured using a superconducting quantum interference device (SQUID) magnetometer (Quantum Design, SQUID-VSM). The *ab initio* calculations of self-consistent geometry optimization of the lattice parameter, the band structure, and the electronic density of states were performed within the density functional theory (DFT) framework, using the program CASTEP in Accelrys software suite.[22,23] The calculations were carried out using the general gradient approximation, Perdew−Burke−Ernzehof (GGA-PBE) functional. Ultrasoft pseudo-potentials were used within the default ultrafine setting.

RESULTS AND DISCUSSION

1. Decomposition of $CaAl_2Si_2$. The ternary Zintl compound $CaAl_2Si_2$ melts congruently at 938 °C under ambient pressure. Under a pressure of 5 GPa, it decomposes to $Ca_2Al_3Si_4$ and aluminum at ~600 °C, as previously reported.[15] In this study, a much higher pressure of 13 GPa has been applied at 750 and 1000 °C for 1 h, and quenched to room temperature within a few minutes. The BSE images of the samples treated at 750 and 1000 °C are shown in Figures 1a and 1b, respectively. At 750 °C, $CaAl_2Si_2$ is decomposed to a mixture of $Ca_2Al_3Si_4$, Al−Si eutectic, and an unidentified phase. At 1000 °C, the $Ca_2Al_3Si_4$ phase almost disappears, and the product is composed of two phases: the unidentified phase and an Al−Si eutectic. The compositions determined by EPMA are shown in Table 1. The compositions of the unidentified phases found in the products from the two different temperatures are very similar: Ca 41.92, Al 20.83, Si 37.49 (total 100.24) in wt %, corresponding to an atomic composition of $CaAl_{0.74}Si_{1.26}$ with Ca:(Al + Si) = 1:2, i.e., $Ca(Al_{0.37}Si_{0.63})_2$. This may suggest that $Ca_2Al_3Si_4$ formed at 750 °C is further decomposed to

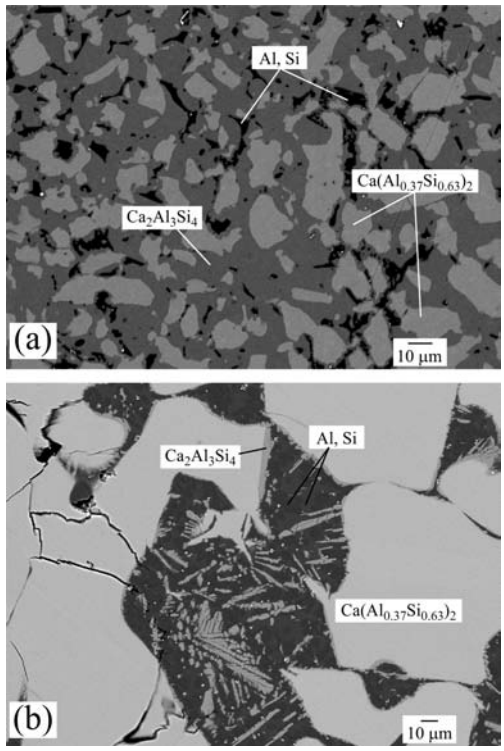

Figure 1. Backscattered electron (BSE) images of the $CaAl_2Si_2$ sample peritectically decomposed under high-pressure and high-temperature (HPHT) conditions of 13 GPa at (a) 750 °C and (b) 1000 °C; EPMA analysis data are shown for some grains with different darknesses.

Table 1. Chemical Compositions Determined by EPMA on the Samples Shown in Figure 1

Conditions			Composition (at. %)		
temperature (°C)	pressure (GPa)	phase	Ca	Al	Si
750	13	Al−Si eutectic	0.01	80.98	19.00
		$Ca_2Al_3Si_4$	22.29	32.13	45.58
		$Ca(Al_{0.37}Si_{0.63})_2$	33.33	24.77	41.89
1000	13	Al−Si eutectic	0.03	82.05	17.92
		$Ca_2Al_3Si_4$	21.62	32.46	45.92
		$Ca(Al_{0.37}Si_{0.63})_2$	33.18	24.49	42.33

$CaAl_{0.74}Si_{1.26}$ + Al−Si eutectic at 1000 °C. Some single crystals of the unidentified compound suitable for X-ray structural analysis were found from the sample treated at 1000 °C, and the structure was determined to be isomorphous with the cubic Laves phase, as shown below.

2. Single-Crystal Analysis. The crystallographic data of $CaAl_{0.74}Si_{1.26}$ is shown in Tables 2 and 3. Some selected bond distances are given in Table 4. The compound is isomorphous with the cubic Laves phase $CaAl_2$ and crystallizes with the space group $Fd\bar{3}m$ (No. 227); the lattice parameter a = 7.754(5) Å and Z = 8. The chemical composition determined by EPMA was used as the occupancy of the 16*c* site in the structural analysis. All of the constituent atoms occupy the special positions, and thus only the atomic displacement parameters and a scale factor were refined. The schematic structural model for $CaAl_{0.74}Si_{1.26}$ is shown in Figure 2.

3. Synthesis from the Ternary Mixtures. The ternary solid solutions $Ca(Al_{1-x}Si_x)_2$ with the cubic Laves phase

dx.doi.org/10.1021/ic400395n | Inorg. Chem. 2013, 52, 6039−6045

Table 2. Details of the Crystal Structure Investigations for $CaAl_{0.74}Si_{1.26}$

parameter	value
formula	$CaAl_{0.74}Si_{1.26}$
formula weight	95.44
crystal system	cubic
space group	$Fd\bar{3}m$ (No. 227)
R_{int}	0.0664
a (Å)	7.754(5)
V (Å^3)	466.2(5)
Z	8
d_{calc}	2.720
temperature (K)	293
λ (Mo Kα) (Å)	0.71073
μ (mm^{-1})	3.175
absorption correction	numerical
θ_{max}	27.130
index ranges	$-9 < h < 6$, $-9 < k, l < 9$
number of total reflections	829
number of unique reflections	39
observed [$I \geq 2\sigma(I)$]	27
number of variables	4
GOF on F_0^2	1.150
$R1/wR2$ [$I \geq 2\sigma(I)$]	0.0202/0.0528
$R1/wR2$ (all data)	0.0287/0.0546
residual density (e$^-$ Å^{-3})	0.222/−0.297

Table 3. Atomic Coordinates and Equivalent Displacement Parameters for $CaAl_{0.74}Si_{1.26}$

atom	site	x	y	z	U_{eq} (Å^2)
Ca	8*b*	5/8	1/8	1/8	0.0182(6)
$Al_{0.74}Si_{1.26}$	16*c*	1/2	1/2	0	0.0178(6)

Table 4. Lattice Parameter a, and Bond Distances for the Cubic Laves Phase Compounds $CaAl_{0.74}Si_{1.26}$, $CaAl_2$, and $CaSi_2$

		Bond Distance (Å)			
CaM_2	a (Å)	Ca−Ca	Ca−M	M−M	ref
$CaAl_{0.74}Si_{1.26}$	7.754(5)	3.358	3.215	2.742	this study
$CaAl_2$	8.04	3.48	3.33	2.84	25
$CaSi_2$	7.59[a]	3.29	3.15	2.68	this study

[a]Calculated by geometrical optimization (see text).

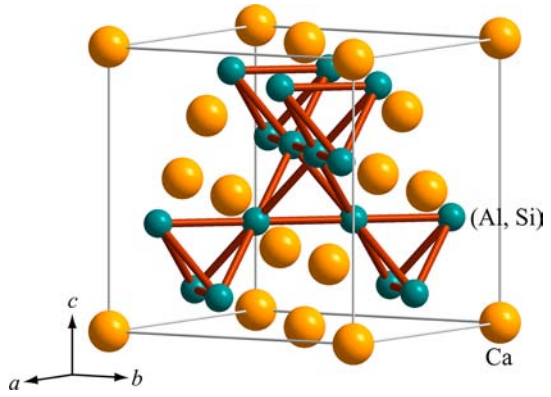

Figure 2. Schematic representation of the structure of the new Laves phase compound, $Ca(Al_{1-x}Si_x)_2$.

structure can be directly prepared from the corresponding ternary mixtures using HPHT conditions of 13 GPa and 1000 °C. Figure 3 shows the XRD pattern of one of the solid

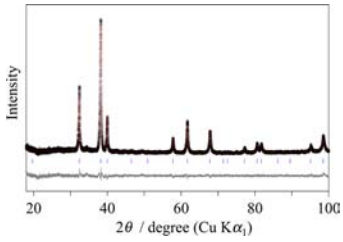

Figure 3. Rietveld analysis of the Laves phase compound $Ca(Al_{0.50}Si_{0.50})_2$ (a = 7.8112(2) Å) based on the powder X-ray diffraction (XRD) pattern measured by an IP Guinier camera (Cu Kα_1). Open circles denote the observed data points, and the solid line represents the calculated diffraction pattern.

solutions $Ca(Al_{0.50}Si_{0.50})_2$ and the Rietveld analysis result. The pattern fits well with the calculated powder pattern based on the single-crystal data given in Table 3. The nominal compositions of the ternary mixtures were almost maintained in the solid solutions obtained by the HPHT treatment. The Laves phase $Ca(Al_{1-x}Si_x)_2$ ($x \leq 0.05$) can be prepared under ambient pressure. The lattice parameters of the solid solutions are plotted against the EPMA compositions x in $Ca(Al_{1-x}Si_x)_2$ in Figure 4, which obey the Vegard's law over the entire range

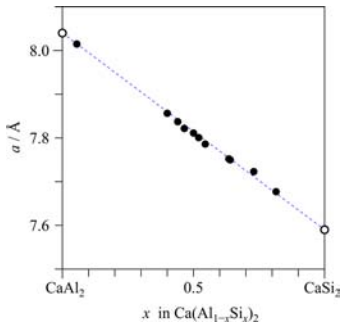

Figure 4. Lattice parameter of the Laves phase solid solutions $Ca(Al_{1-x}Si_x)_2$ versus silicon content (x). The lattice parameters of the end members $CaAl_2$ and $CaSi_2$ are given in Table 4.

between $CaAl_2$ and $CaSi_2$. The preparation of the binary Laves phase $CaSi_2$ has been attempted using a similar HPHT condition of 13 GPa and 1000 °C. However, the starting $CaSi_2$ was transformed to a high-pressure polymorph, the tetragonal $CaSi_2$ that is isomorphous with the α-$ThSi_2$ structure.[24] When a higher pressure of 15 GPa at 1000 °C was used, a different binary compound $CaSi_3$ was obtained.[6] The lattice parameter of the hypothetical binary Laves phase compound $CaSi_2$ was estimated to be a = 7.590 Å by geometry optimization using CASTEP. This lattice parameter is employed in Figure 4 as an end member. Note that the Vegard's law for the solid solution $Ca(Al_{1-x}Si_x)_2$ can be extended over the entire compositional range between the coupled end members, $CaAl_2$ and $CaSi_2$. Although we have not yet succeeded in the preparation of the Laves phase compound $CaSi_2$, the expected lattice parameter used in Figure 4 should be reasonable.

The lattice parameters and bond distances of calcium-containing Laves phase compounds with various metals, CaM_2

dx.doi.org/10.1021/ic400395n | Inorg. Chem. 2013, 52, 6039−6045

(M = Al, Ni, Rh, Pd, Ir, Pt, Li) found in a crystallographic database[25] are compared with those of $CaSi_2$ in Figure 5. Since

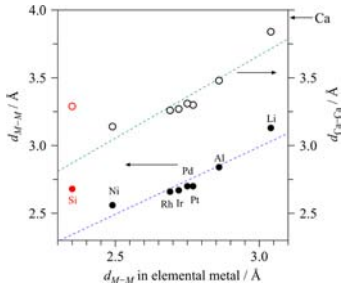

Figure 5. Bond distances d_{M-M} (M−M) (solid circles, ●) and d_{Ca-Ca} (Ca−Ca) (open circles, ○) of some calcium-containing Laves phase compounds CaM_2 against the shortest M−M distance in the corresponding elemental metals; the values for $CaSi_2$ are taken from Table 4.

the Ca and the metal (M) atoms occupy the special positions, the atomic distances Ca−Ca and M−M can be calculated from the lattice parameter a: $d_{M-M} = (\sqrt{2}/4)a$, and $d_{Ca-Ca} = (\sqrt{3}/4)a$, respectively. These atomic distances are compared with those of the corresponding metal elements in the figure. Note that, in the Laves phase CaM_2, the atomic distance M−M is very close to those of the elemental metals. The Ca−Ca atomic distances of the Laves phase CaM_2 are shorter than that of calcium metal. This can be interpreted in terms of the electronegativity difference between Ca and M. The electronegativity of M atoms is larger than that of the Ca atom (except Li). The Ca atom is partially ionized. Note that the Si−Si distance in $CaSi_2$ (2.68 Å) is longer than that of the covalent distance Si−Si (2.35 Å) in the diamond structure. According to the Mulliken charge calculation by CASTEP, the charge distribution in the Laves phase $CaSi_2$ is $Ca^{+0.79}(Si^{-0.40})_2$. The large electronegativity difference between Ca and Si appears to be the reason of the long Si−Si distance in the Laves phase structure. The Si atoms in the Laves phase $CaSi_2$ are 6-coordinated, similar to the high-pressure polymorph of silicon with the β-tin structure.

4. Superconductivity. The temperature dependence of the magnetic susceptibility of the sample $Ca(Al_{0.50}Si_{0.50})_2$ measured under a magnetic field of 2.5 Oe is shown in Figure 6. A clear superconducting transition was observed at T_c = 2.6 K. The inset of the figure shows the magnetization curve of the same sample. This is a Type II superconductor; the lower critical field (H_{c1}) is as low as 5 Oe. The magnetic susceptibility of the solid solutions were measured using zero field cooling (ZFC) and field cooling (FC) modes under a magnetic field of 2.5 Oe, which is lower than the H_{c1} = 5 Oe magnetic field. Figure 7 shows the T_c and the superconducting volume fraction of the solid solutions $Ca(Al_{1-x}Si_x)_2$ estimated from the FC mode at 1.9 K against the silicon content (x). Although the T_c is almost constant at 2.6 K over the solid solutions, the Meissner exclusion volume abruptly decreases with a deviation from the stoichiometric composition CaAlSi. This finding indicates that only the solid solution having a composition of $Ca(Al_{1-x}Si_x)_2$ with x very close to 0.5 can become a superconductor. As will be discussed later, it is an interesting issue why only the Laves phase compound with the stoichiometric composition shows superconductivity specifically. The temperature dependence of the upper critical field ($H_{c2}(T)$) was determined from the

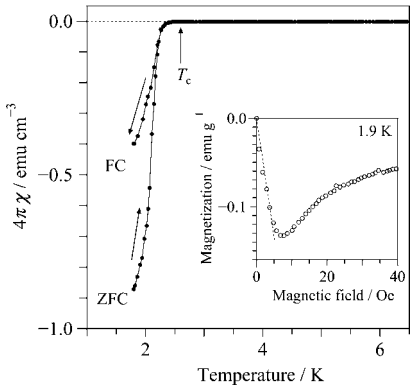

Figure 6. Temperature dependence of the magnetic susceptibility of $Ca(Al_{0.50}Si_{0.50})_2$ measured in zero field cooling (ZFC) and field cooling (FC) processes under a magnetic field strength of 2.5 Oe. The inset shows dc magnetization of the same sample at 1.9 K, versus magnetic field strength.

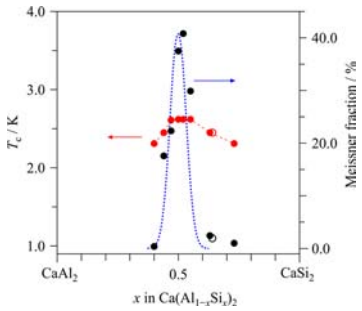

Figure 7. T_c and Meissner volume fraction of the Laves phase solid solutions $Ca(Al_{1-x}Si_x)_2$ as a function of Si content x. The open circles show the values of the $CaAl_2Si_2$ decomposed under HPHT and left for 3 months under ambient pressure.

temperature dependence of the magnetization under varying magnetic field strengths up to 7 T; this is shown in Figure 8.

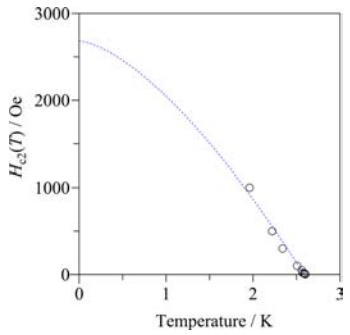

Figure 8. Temperature dependence of $H_{c2}(T)$ of the Laves phase compound Ca(AlSi). The dotted line shows the WHH relationship to estimate $H_{c2}(0)$.

The initial slope (dH_{c2}/dT) at T_c is calculated to be 1500 Oe/K. We assume the Werthamer−Helfand−Hohenberg (WHH) relation

$$H_{c2}(0) = 0.693\left(-\frac{dH_{c2}}{dT}\right)\Big|_{T_c} T_c$$

dx.doi.org/10.1021/ic400395n | Inorg. Chem. 2013, 52, 6039−6045

for the Type II superconductor in a dirty limit;[26] the $H_{c2}(0)$ value is estimated to be ~2700 Oe. The coherence length (ξ) is calculated to be ~35 nm, using a relation of

$$H_{c2}(0) = \frac{\Phi_0}{2\pi\xi^2}$$

where Φ_0 is the flux quantum. These values are comparable to those of the layer-structured CaAlSi, which is considered to be a weak-coupling BCS superconductor.[27]

Superconductivity of transition-metal Laves phases has been extensively studied such as AB_2 (A = Ca, Sr, Sc, Y, La, Zr, Hf, Th, Lu; B = V, Mo, Re, Ru, Os, Rh, Ir, Pt, Te).[28−30] Most of the compounds are composed of transition metals. Note that the compound of the present study does not include transition metals, but contains a (Si,Al) covalent network.

As described above, the Zintl compound $CaAl_2Si_2$ is decomposed to a mixture of the Laves phase compound $Ca(Al_{0.37}Si_{0.63})_2$ and an Al−Si eutectic at 13 GPa and 1000 °C. Figure 9 shows the time dependence of the magnetic

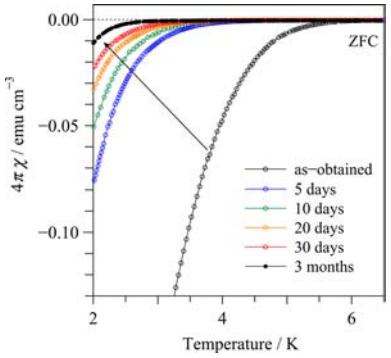

Figure 9. Temperature dependence of the magnetic susceptibility in ZFC mode of the $CaAl_2Si_2$ decomposed under a pressure of 13 GPa at 1000 °C.

susceptibility in ZFC mode of the decomposed product. The as-prepared sample obtained after the HPHT treatment shows a superconducting transition at T_c = 6 K, which is higher than that (T_c = 2.6 K) of the ternary Laves phase compounds. As can be seen from the figure, the superconducting volume fraction and the T_c value decrease with time, and after 3 months, the T_c value has decreased to ~2.5 K, corresponding to that of the Laves phase compound. The T_c and the superconducting Meissner volume fraction measured on the decomposed sample after 3 months are shown in Figure 7 by open circles, together with the values of the solid solutions.

It is well-known that the superconductivity of Al metal is enhanced by supersaturation of Si in the Al−Si binary system by means of rapid solidification under high pressure.[31,32] The T_c value of aluminum increases from 1.2 K to 6.2 K for Al−30 at. % Si. It is very likely that the superconductivity with T_c = 6 K of the $CaAl_2Si_2$ peritectically decomposed under pressure is due to the presence of the Al−Si eutectic phase, in which aluminum is supersaturated with silicon. While the sample is maintained under ambient pressure, Si supersaturated in Al is released, and the T_c value decreases, coupled with the decrease of the superconducting volume fraction. The lattice parameter of the Laves phase compound was found to be essentially unchanged with time, and moreover, the superconducting volume fraction of the Laves phase samples synthesized from the ternary mixture $Ca(Al_{1-x}Si_x)_2$ as single phase without the Al−Si eutectic phase are unchanged, even after 4 months.

5. Structural Consideration of the New Laves Phase Compound with a Stoichiometric Composition CaAlSi. The ternary silicide CaAlSi isomorphous with the AlB_2 type layered structure is known as a superconductor with T_c = 7.7 K.[17] The layer structured CaAlSi is also isomorphous with the high-T_c superconductor MgB_2 (T_c = 39 K).[33] The Laves phase compound CaAlSi of the present study is a new polymorph of the high-pressure phase. In the preparation of the high-pressure phase with the stoichiometric composition, we have prepared the layered compound CaAlSi first, and treated it under HPHT conditions. In the layered polymorph, Si and Al atoms are completely ordered in the *ab* plane, such as B and N in *h*-BN, and stacked with Ca atoms between the layers with or without a superlattice along the *c*-axis.[27,34] In the Laves phase CaAlSi, the structure can be regarded as being composed of Al_2Si_2 tetrahedra by corner sharing, as shown in Figure 2, the Ca atoms being placed in the space formed by the Al_2Si_2 tetrahedral network; Ca atoms have the same arrangement as in the diamond. In the layered CaAlSi, the network consists of only Al−Si sp^2 bonds, while in the Laves phase compound, the tetrahedral unit $[Al_2Si_2]$ contains Si−Si, Al−Al, and Al−Si bonds. There are many possible ways to connect the $[Al_2Si_2]$ tetrahedra in a three-dimensional (3D) network. The $[Al_2Si_2]$ tetrahedral units should have 3-fold symmetries in the unit cell with space group $Fd\bar{3}m$, and, at the same time, the tetrahedra should be linked by sharing corners, maintaining the stoichiometric composition CaAlSi. It is difficult to make an ordered structure, even if a very large super cell is used. We are tentatively assuming an averaged structure. The hybridization of the *s*/*p* orbitals between Si−Si Al-Al, and Al−Si must be taken into account. The *s*/*p* orbitals of the covalent network should also be hybridized with Ca orbitals. It is an interesting but difficult issue why only the Laves phase compound with the stoichiometric composition CaAlSi shows the superconductivity among the solid solutions $Ca(Al_{1-x}Si_x)_2$ with widely varying silicon and aluminum contents.

If we focus on the environment of the Ca atoms, the structure can be regarded as being composed of large Al and Si tetrahedral cages @Al_6Si_6 with all of the four corners truncated, as shown in Figure 10. These are linked by face sharing with each other, with Ca atoms being placed at the center of the large truncated tetrahedral cages. The structure can be regarded

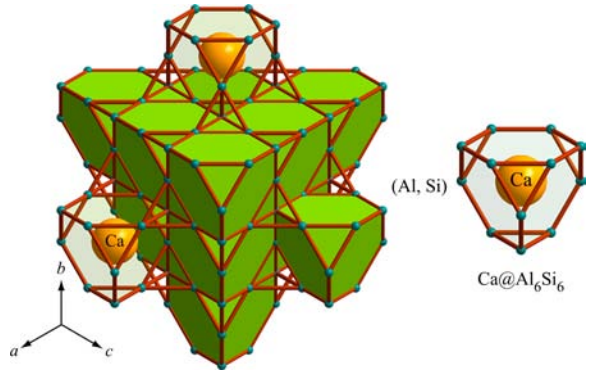

Figure 10. Schematic structural illustration of the Laves phase compound Ca(AlSi) composed of truncated tetrahedral cages with Ca atoms in the center, Ca@Al_6Si_6.

dx.doi.org/10.1021/ic400395n | Inorg. Chem. 2013, 52, 6039−6045

as a type of clathrate structure composed of new clathrate cages $Ca@Al_6Si_6$.

6. Electronic Band Structure. The electronic band structures of the two types of Laves phase compounds $CaAl_2$ and $CaSi_2$ were calculated based on the crystallographic data given in Tables 3 and 4, using CASTEP. The structure of $CaSi_2$ was estimated by geometrical optimization, as described previously. The electron densities of states (DOS) thus obtained are compared in Figure 11. The band structure $[Si_2]$

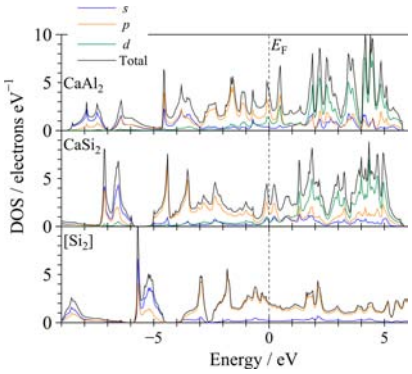

Figure 11. Electronic density of states (DOS) for $CaAl_2$, $CaSi_2$, and $[Si_2]$ with the cubic Laves phase structure calculated using CASTEP software.

with the Laves phase structure without containing Ca has been calculated, and its DOS is compared with that of $CaSi_2$ in the figure. The $[Si_2]$ has a metallic band structure with nonzero DOS at the Fermi level. The profile of the DOS of $CaSi_2$ is much different from that of $[Si_2]$, implying that the band structure of $CaSi_2$ cannot be discussed from a rigid band model, unlike clathrate compounds. This is due to the strong hybridization of the Ca 3*d* orbitals and the Si 3*p* orbitals near the Fermi level. In the calculation of the band structure of the Laves phase CaAlSi, we need information on the distribution of Al and Si atoms in the network. It should also be hybridized with the Ca 3*d* orbitals, and would be more complicated. We are tentatively estimating that the band structure of the Laves phase CaAlSi can be an intermediate, or averaged one between those of $CaAl_2$ and $CaSi_2$. Neutron diffraction and theoretical studies are required.

CONCLUSIONS

A new ternary Laves phase compound $Ca(Al_{1-x}Si_x)_2$ ($0.35 \leq x \leq 0.75$) has been prepared using a high-pressure and high-temperature (HPHT) condition of 13 GPa at 1000 °C. The lattice parameters of the ternary solid solutions can fit on a linear line tying the parameters of $CaAl_2$ and $CaSi_2$. The stoichiometric compound CaAlSi shows superconductivity at T_c = 2.6 K. The Laves phase compound with a covalent network can be regarded as a type of clathrate compound composed of truncated tetrahedra with Ca atoms in the center, $Ca@Al_6Si_6$.

ASSOCIATED CONTENT

Supporting Information

CIF file for $Ca(Al_{0.37}Si_{0.63})_2$. This material is available free of charge via the Internet at http://pubs.acs.org.

AUTHOR INFORMATION

Corresponding Author

*E-mail: syamana@hiroshima-u.ac.jp.

Notes

The authors declare no competing financial interest.

ACKNOWLEDGMENTS

This work has been supported by the Japan Society for the Promotion of Science (JSPS) through its "Funding Program for World-Leading Innovative R&D on Science and Technology (FIRST) Program".

REFERENCES

(1) Yamanaka, S.; Enishi, E.; Fukuoka, H.; Yasukawa, M. *Inorg. Chem.* **2000**, *39*, 56−58.
(2) Yamanaka, S.; Izumi, S.; Maekawa, S.; Umemoto, K. *J. Solid State Chem.* **2009**, *182*, 1991−2003.
(3) Rachi, T.; et al. *Phys. Rev. B* **2005**, *72*, 144504.
(4) Yamanaka, S.; Maekawa, S. *Z. Naturforsch. B* **2006**, *61*, 1493−1499.
(5) Wosylus, A.; Prots, Y.; Burkhardt, U.; Schnelle, W.; Schwarz, U.; Grin, Y. *Z. Naturforsch. B* **2006**, *61*, 1485−1492.
(6) Schwarz, U.; Wosylus, A.; Rosner, H.; Schnelle, W.; Ormeci, A.; Meier, K.; Baranov, A.; Nicklas, M.; Leipe, S.; Müller, C. J.; Grin, Y. *J. Am. Chem. Soc.* **2012**, *134*, 13558−13561.
(7) Fukuoka, H.; Yamanaka, S. *Phys. Rev. B* **2003**, *67*, 094501.
(8) Fukuoka, H.; Baba, K.; Yoshikawa, M.; Ohtsu, F.; Yamanaka, S. *J. Solid State Chem.* **2009**, *182*, 2024−2029.
(9) Fukuoka, H.; Tomomitsu, Y.; Inumaru, K. *Inorg. Chem.* **2011**, *50*, 6372−6377.
(10) Schnelle, W.; Ormeci, A.; Wosylus, A.; Meier, K.; Grin, Y.; Schwarz, U. *Inorg. Chem.* **2012**, *51*, 5509−5511.
(11) Imai, M.; Kikegawa, T. *Chem. Mater.* **2003**, *15*, 2543−2551.
(12) Hao, J.; Zou, B.; Zhu, P.; Gao, C.; Li, Y.; Liu, D.; Wang, K.; Lei, W.; Cui, Q.; Zou, G. *Solid State Commun.* **2009**, *149*, 689−692.
(13) Yu, F.; Sun, J.-X.; Yang, W.; Tian, R.-G.; Ji, G.-F. *Solid State Commun.* **2010**, *150*, 620−624.
(14) Ji, S.; Tanaka, M.; Zhang, S.; Yamanaka, S. *Inorg. Chem.* **2012**, *51*, 10300−10305.
(15) Tanaka, M.; Zhang, S.; Tanaka, Y.; Inumaru, K.; Yamanaka, S. *J. Solid State Chem.* **2013**, *198*, 445−451.
(16) Nakano, H.; Yamanaka, S. *J. Solid State Chem.* **1994**, *108*, 260−266.
(17) Imai, M.; Nishida, K.; Kimura, T.; Abe, H. *Appl. Phys. Lett.* **2002**, *80*, 1019−1021.
(18) Kawai, N.; Endo, S. *Rev. Sci. Instrum.* **1970**, *41*, 1178−1181.
(19) Sheldrick, G. M. *Program for Structure Refinement*; University of Göttingen, Germany, 1997.
(20) Farrugia, L. J. *J. Appl. Crystallogr.* **1999**, *32*, 837−838.
(21) Coelho, A. *TOPAS-Academic V4.1: General profile and structure analysis software for powder diffraction data*; Coelho Software: Brisbane, Australia, 2007.
(22) CASTEP is available from Accelrys, San Diego, CA (http://www.accelrys.com).
(23) Segall, M. D.; Lindan, P. J. D.; Probert, M. J.; Pickard, C. J.; Hasnip, P. J.; Clark, S. J.; Payne, M. C. *J. Phys.: Condens. Matter.* **2002**, *14*, 2717.
(24) Silverman, M. S.; Soulen, J. R. *J. Phys. Chem.* **1963**, *67*, 1919−1920.
(25) Inorganic Crystal Structure Database (ICSD), Fachinformationzentrum (FIZ) Karlsruhe and the National Institute of Standards and Technology (NIST).
(26) Werthamer, N. R.; Helfand, E.; Hohenberg, P. C. *Phys. Rev.* **1966**, *147*, 295.
(27) Kuroiwa, S.; Sagayama, H.; Kakiuchi, T.; Sawa, H.; Noda, Y.; Akimitsu, J. *Phys. Rev. B* **2006**, *74*, 014517.

(28) Matthias, B. T.; Geballe, T. H.; Compton, V. B. *Rev. Mod. Phys.* **1963**, *35*, 1−22.
(29) Phillips, J. C. *Physics of High-T_c Superconductors*; Academic Press: New York, 1989.
(30) Vonsovsky, S. V.; Izyumov, Y. A.; Kurmaev, E. Z. *Superconductivity in Transition Metals*; Springer, New York, 1982.
(31) Degtyareva, V. F.; Chipenko, G. V.; Ponyatovskii, E. G.; Rashchupkin, V. I. *Sov. Phys. Solid State* **1984**, *26*, 733−734.
(32) Chevrier, J.; Pavuna, D.; Cyrot-Lackmann, F. *Phys. Rev. B* **1987**, *36*, 9115−9121.
(33) Nagamatsu, J.; Nakagawa, N.; Muranaka, T.; Zenitani, Y.; Akimitsu, J. *Nature* **2001**, *410*, 63−64.
(34) Sagayama, H.; Wakabayashi, Y.; Sawa, H.; Kamiyama, T.; Hoshikawa, A.; Harjo, S.; Uozato, K.; Ghosh, A. K.; Tokunaga, M.; Tamegai, T. *J. Phys. Soc. Jpn.* **2006**, *75*, 043713.

dx.doi.org/10.1021/ic400395n | *Inorg. Chem.* 2013, 52, 6039−6045